NASA Technical Memorandum 109118

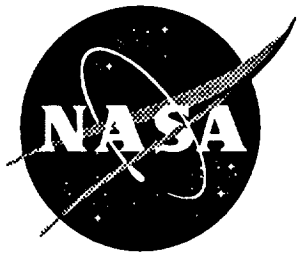

Evaluation of Several Non-reflecting Computational Boundary Conditions for Duct Acoustics

Willie R. Watson and William E. Zorumzki
Langley Research Center, Hampton, Virginia

Steve L. Hodge
Virginia Consortium of Engineering and Science Universities, Hampton, Virginia

May 1994

National Aeronautics and
Space Administration
Langley Research Center
Hampton, Virginia 23681-0001

Evaluation of Several Non-reflecting Computational Boundary Conditions for Duct Acoustics

Willie R. Watson and William E. Zorumski
NASA Langley Research Center, Hampton Virginia 23666
Steve L. Hodge
Virginia Consortium of Engineering and Science Universities, Hampton Virginia 23666

Abstract

Several non-reflecting computational boundary conditions that meet certain criteria and have potential applications to duct acoustics are evaluated for their effectiveness. The same interior solution scheme, grid, and order of approximation are used to evaluate each condition. Sparse matrix solution techniques are applied to solve the matrix equation resulting from the discretization. Modal series solutions for the sound attenuation in an infinite duct are used to evaluate the accuracy of each non-reflecting boundary condition. The evaluations are performed for sound propagation in a softwall duct, for several sources, sound frequencies, and duct lengths. It is shown that a recently developed nonlocal boundary condition leads to sound attenuation predictions considerably more accurate than the local ones considered. Results also show that this condition is more accurate for short ducts. This leads to a substantial reduction in the number of grid points when compared to other non-reflecting conditions.

1 Introduction

Over the past decade, there has been considerable interest in the use of computational methods for obtaining solutions to problems in aeroacoustics. This interest stems primarily from a lack of exact analytical solutions for predicting, understanding, and controlling various acoustic phenomena. As computational models have evolved, difficulty with the closure of the computational domain has emerged as a major problem in the calculations.

The difficulty with closure of the computational domain arises because aeroacoustics problems are typically set in an infinite domain with a radiation condition on the boundary surface at infinity. However the computational domain cannot extend to infinity, so the problem is decomposed into a finite computational domain within some outer domain that extends to the boundary at infinity. The interface between these domains is called the artificial or computational boundary. One needs a set of equations valid at this computational

boundary. The primary purposes of these equations is to guarantee a unique and well-see posed solution to the aeroacoustics problem. These equations are usually a set of partial differential operators whose terms involve only local information at each boundary point such as the dependent variables and their derivatives. To avoid nonphysical reflections from occurring at the computational boundary, these differential operators are also intended to constrain the local solution to consist of waves traveling outward from the computational domain. When used in this manner, the differential equations are called local non-reflecting boundary conditions.

There currently exist a large number of research papers concerned with the development of local non-reflecting conditions for use at computational boundaries (refs. [1]- [6]). The references cited above represent only a small sampling of local boundary conditions, which have potential application to duct acoustics. Unfortunately, experiences show that the conditions developed in these works are reflecting for a large class of aerocoustic problems. This is especially true for classes of aeroacoustic problems for which waves impinging on the computational boundary is not close to normal incidence.

The proper approach to dealing with the problem of finite computational domains is to match the computational solution in the inner domain with the general solution in the outer domain. This general outer solution satisfies the radiation condition at infinity and constrains the solution on the computational interface. But this constraint is not in general a local condition. Instead, a given value of a variable at one point on the interface surface influences the values of other variables at all points on the interface surface. Constraints of this type are call nonlocal conditions. They can be constructed for all classes of problems in which the exterior domain is linear.

In a recent report (ref. [7]), the authors presented the formulation of a nonlocal non-reflecting boundary condition for duct acoustics. The purpose of this paper is to compare this nonlocal boundary condition to several local conditions that could compete with it. Due to space limitation and time restraints, all of the existing non-reflecting boundary conditions could not be compared with this new condition. To limit the number of choices, we include only those conditions that meet certain criteria.

Section 2 defines the basic equations used in the computation and presents the non-reflecting boundary conditions that are tested. Modal series solutions for the sound attenuation in an infinite duct are used to evaluate the accuracy of each boundary condition. This series solution is also presented in section 2. The interior solution technique, method of implementing each boundary condition, effect of each condition on the matrix structure, and matrix solution technique is described in section 3. Results for a broad range of acoustic parameters are presented in section 4. Conclusions, relative to boundary conditions evalu-

ated in this paper are given in section 5. References and figures cited in this report are given at the end of section 5.

2 Governing Equations and Boundary Conditions

Consider a two-dimensional rectangular duct without mean flow as shown in figure 1. The duct is assumed infinitely long in the axial direction with a known acoustic source pressure at the plane $x = 0$. The walls of the duct contain sound absorbing material whose material properties vary along the axis of the duct for $0 \leq x \leq L$. Sound absorbing properties of the wall lining are specified by perscribing the admittance of the lower wall, $\beta_0(x)$, and upper wall, $\beta_H(x)$, of the duct. Within the region $L < x \leq \infty$ the material properties of the liner are assumed uniform, so that an outgoing wave field exists in this region. It is the purpose of this work to test several non-reflecting boundary conditions for terminating the duct at $x = L$.

Steady-State acoustic wave solutions within the duct in figure 1, take the form

$$\tilde{p}(x, y, t) = p(x, y)e^{i2\pi ft} \tag{1}$$

where $\tilde{p}$ is the steady state acoustic pressure, f is the frequency in Hertz, $i = \sqrt{-1}$, and $p(x, y)$ satisfies Helmholtz's equation

$$\nabla^2 p + k^2 p = 0 \tag{2}$$

Here, $k = \frac{2\pi f}{c}$ is the freespace wavenumber, c is the sound speed and ∇^2 is the Laplace operator in the (x, y) plane.

The inflow and wall boundary conditions require a specification of the source pressure and wall admittance

$$p(0, y) = G(y) \tag{3}$$

$$\frac{\partial p}{\partial y}(x, 0) = -ik\beta_o(x)p(x, 0) \tag{4}$$

$$\frac{\partial p}{\partial y}(0, H) = ik\beta_H(x)p(x, H) \tag{5}$$

where $G(y)$, $\beta_0(x)$, and $\beta_H(x)$ denote the known source pressure and normalized admittance of the lower and upper wall respectively. To complete the specification of the boundary value problem in the duct, a non-reflecting condition must be specified at the outflow boundary.

Several non-reflecting boundary conditions were considered for application at $x = L$. In order to limit the number of choices only those boundary conditions that met the following criteria were considered

1. The boundary condition must have a frequency and possibly time domain extension.

2. The boundary condition must be extendible to shearing flows and three dimensionality.

3. The order of the boundary condition must be such that the linear finite element theory of ref. [7] could be applied for the interior solution.

4. The coupling of the boundary condition with the interior solution scheme must lead to a coefficient matrix that remains block tridigonal.

The non-reflecting conditions that meet the above criteria that are tested in this paper are

1. The local boundary condition of Giles (ref. [5])

$$\frac{1}{c}\frac{\partial \tilde{p}}{\partial t} + \frac{\partial \tilde{p}}{\partial x} = 0 \tag{6}$$

2. The nonlocal frequency-domain boundary condition of the current authors (ref. [7])

$$\{p_i\} = [Z_{ij}]\{u_j\} \tag{7}$$

where $\{p_i\}, \{u_j\}$ are vectors containing values of the frequency-domain acoustic pressure and normal velocity at boundary node i and j respectively. Further, the coefficients in the nodal impedance matrix $[Z_{ij}]$ are defined explicitly in ref. [7].

3. The local highly-absorbing boundary condition of Engquist and Majda (ref. [1])

$$-\frac{1}{c^2}\frac{\partial^2 \tilde{p}}{\partial t^2} - \frac{1}{c}\frac{\partial^2 \tilde{p}}{\partial x \partial t} + \frac{1}{2}\frac{\partial^2 \tilde{p}}{\partial y^2} = 0 \tag{8}$$

Several remarks concerning the above boundary conditions are in order. Each of the above boundary conditions has been specialized to both a no-flow environment and right moving waves. All of the above conditions are non-reflecting for plane wave sources. The first non-reflecting condition above is a familiar one that was derived by Hedstrom (ref. [2]) and several others prior to the work of Giles. This condition has been used by duct acousticians for several decades as a termination condition, and is often referred to as the ρc termination condition. Because the Giles condition (ref. [5]) in the absence of mean flow reduces to this condition, it is referred to here as the "Giles condition." Finally, Engquist and Majda ((ref. [1]) have shown that the third condition gives reflections considerably smaller than the first condition when the Neumann wall boundary condition is imposed. This conclusion may not be valid when the sound propagates between walls lined with sound absorbing material.

Periodic acoustic fields determined from the non-reflecting boundary conditions above are used to evaluate the performance of the wall lining over x length of linings. The following expression is used to evaluate the acoustic intensity at a point (x,y) in the duct ref. ([8])

$$I(x,y) = \frac{1}{4\pi f \rho_0} \Re \left\{ p(x,y) \left[i \frac{\partial p(x,y)}{\partial x} \right]^* \right\} \tag{9}$$

where the superscript asterisk denotes the complex conjugate, ρ_0 is the mean density within the duct, and $\Re\{\ \}$ denotes the real part of the complex expression within the braces. The attenuation over x length of lining in decibels is

$$dB(x) = 10 log_{10} \frac{W(0)}{W(x)} \tag{10}$$

$$W(x) = \int_0^H I(x,y) dy \tag{11}$$

Modal series solutions for the attenuation are used to determine the accuracy of each non-reflecting boundary condition. These series solutions are possible when the material properties of the wall lining are constant. When this condition is met, the solutions to Helmholtz's equation in the form of outgoing waves are of the complex exponential form

$$\tilde{p}(x,y) = \sum_{m=1}^{M} A_m P_m(y) e^{iK_m x} \tag{12}$$

where K_m is the axial propagation constant, and the functions $P_m(y)$ are the acoustic pressure eigenfunctions. Note that the series has been truncated at a finite number M. To insure no reflections, the sum in equation (12) is taken only over modes whose axial propagation constants possess positive imaginary parts. The method for obtaining P_m and K_m is described in ref. [7] and the mode amplitude coefficients are obtained from the source condition and the orthogonality of the lined duct modes

$$A_m = \frac{\int_0^H G(y) P_m(y) dy}{\int_0^H P_m^2(y) dy} \tag{13}$$

Equations (12) and (13) are substituted into equations (9)-(11) to obtain the modal series expression for the attenuation of the lining.

3 The Numerical Method

In this section of the paper we describe the interior solution technique, the numerical implementation of each of the non- reflecting boundary conditions, and the matrix solution technique. Several details have been purposely omitted since they can be obtained in several of the cited references.

3.1 The Interior Solution Technique

The numerical method chosen to solve equation 2 coupled with the source, wall and non-reflecting boundary conditions is a Galerkin Finite Element Method with linear elements used as the basis functions. The method is described in detail in the earlier paper (ref. [7]). Application of the method results in a matrix equation of the form

$$[A]\{\Phi\} = \{F\} \tag{14}$$

where $[A]$ is an $MNxMN$ complex matrix, and $\{\Phi\}$ is a $MNx1$ column vector containing the nodal values of the unknown acoustic pressure. The integers N and M are the number of grid points in the x and y direction respectively. Equation (14) does not contain the effects of the non-reflecting condition. The non-reflecting condition must be imposed on this matrix equation before the solution can be obtained. Details of the implementation of each non-reflecting boundary condition are now discussed.

3.2 Boundary Condition Implementation

The frequency-domain form of the Giles condition ref. [5] is

$$k\,p(L,y) - i\frac{\partial p(L,y)}{\partial x} = 0 \tag{15}$$

The Giles condition is discretized as followed

$$k\,p_{N,j} - i\frac{[p_{N,j} - p_{N-1,j}]}{(x_N - x_{N-1})} = 0, \qquad j = 1,2...M \tag{16}$$

Note that the spatial gradient in the boundary condition discretization is only first order accurate. Thus, the interior solution and boundary condition discretization are of the same order. Equation 16 constitutes M equations which are imposed as restraints on equation 14 prior to solving the matrix equation.

Boundary condition implementation of the nonlocal condition is exactly as discussed in ref. [7]. The axial velocity vector at the grid points $\{u_j\}$ is expressed in terms of the gradient of the acoustic pressure field. The axial acoustic pressure gradient is then discretized with a first order difference approximation. This results in M restraint equations which are imposed on the matrix equation in the usual manner.

The frequency-domain form of the Engquist and Majda condition ref. [1] is

$$k^2 p(L,y) - ik\frac{\partial p(L,y)}{\partial x} + \frac{1}{2}\frac{\partial^2 p(L,y)}{\partial y^2} = 0 \tag{17}$$

For the numerical experiment presented here, the above equation is discretized using first order one-side differences

$$k^2 p_{N,j} - ik\frac{[p_{N,j} - p_{N-1,j}]}{(x_N - x_{N-1})} + \frac{[p_{N,j+2} - 2p_{N,j+1} + p_{N,j}]}{2(y_{j+1} - y_j)^2} = 0, \quad j = 1, 2...M-2 \tag{18}$$

$$k^2 p_{N,j} - ik\frac{[p_{N,j} - p_{N-1,j}]}{(x_N - x_{N-1})} + \frac{[p_{N,j-2} - 2p_{N,j-1} + p_{N,j}]}{2(y_j - y_{j-1})^2} = 0, j = M-1, M \tag{19}$$

Note that although the boundary condition has a second derivative term in y, first order one-sided differences are still used to approximate all derivatives in x and y. The M equations generated by the discretization aboved are imposed on the matrix equation (14) as a set of restraints.

3.3 Effects of Boundary conditions on the Matrix Structure

The augmented global matrix generated by Galerkin's Method, following application of the source, wall, and non-reflecting boundary conditions, is an unsymmetric, positive indefinite, complex matrix. Fortunately, owing to the discretization scheme and choice of non-reflecting boundary conditions, it will be block tridiagonal as shown in figure 2. The superscript T denotes the matrix transpose in the figure. Each minor block A_I and B_I are MxM matrices that are tridiagonal. These blocks are obtained from the interior solution scheme and wall boundary conditions. The minor block E_1 is the identity matrix, which results from applying the source condition (3). Minor blocks C_N and D_N are MxM complex matrices that contain the effects of the non-reflecting conditions. Each minor block C_N and D_N is a diagonal matrix when the Giles condition (16) is implemented. Application of the Engquist and Majda condition (18) and (19) leads to a diagonal minor block C_N, while D_N will contain a main diagonal, two superdiagonal, and two subdiagonals. Finally, both minor blocks are full matrices when the nonlocal condition of Zorumski, Watson, and Hodge (7) is implemented.

3.4 Solution to the Matrix Equation

The matrix $[A]$, generated by the method described here, is not symmetric or positive definite. Fortunately, it is block tridiagonal as shown in figure 2. Much practical importance arises from this structure, as it is convenient for minimizing storage and maximizing computational efficiency. Economy of storage is acheived by storing the rectangular array of coefficients within the bandwidth of $[A]$ as shown in figure 3. All computation, storage and boundary condition implementation is performed only on the rectangular portion of this matrix. Special matrix techniques exist for a solution of this structure. Gaussian elimination with partial pivoting and equivalent row infinity norm scaling is used to reduce the rectangular system to

upper triangular form. Back substitution is then used to obtain the solution for the acoustic pressure.

4 Results and Discussion

A computer code implementing all three boundary conditions and the modal series solution discussed in this paper has been developed and programmed to run on a supercomputer. The results were obtained with the underlying objective of comparing the attenuation obtained from each boundary condition with the modal series solutions over a broad range of acoustic parameters. The same interior solution scheme, grid, and order of approximation are used to evaluate each non-reflecting condition. Within this context, the effect of changing the source pressure, frequency and duct length is evaluated for a specified lining.

With respect to the acoustic parameters, effects of three source pressures on the boundary condition are studied (see eq. 12)

$$G(y) = P_1(y) \tag{20}$$

$$G(y) = P_5(y) \tag{21}$$

$$G(y) = \sum_{m=1}^{10} m^2 P_m(y) \tag{22}$$

Other parameters include a softwall duct with ($\beta_0 = \beta_H = .5 - .5i$), three frequencies ($f = 100\ Hz$, $f = 1,000\ Hz, f = 5,000\ Hz$) and four duct lengths ($L = H$, $L = .8H$, $L = .6H$, $L = .2H$). All calculations were performed for a duct 1 meter high ($H = 1\ m$) and at ambient conditions ($c = 343\ m/sec$). The griding remained fixed as each acoustic parameter was changed. Fifty-one evenly spaced points were used in the y direction ($M = 51$) and the number of axial points N was determined such that 10 points per axial wavelength were retained at the highest frequency of 5,000 Hz.

Figure 4 compares the attenuations predicted from the boundary conditions when the location of the boundary is at $L = H$. The source is the lowest order mode and the frequency is 100 Hz. The new nonlocal condition give predictions that are in excellent agreement with the modal series. Giles's condition is more accurate than the condition of Engquist and Majda for $\frac{x}{L} < .65$, and in the region $\frac{x}{L} > .65$ the condition of Engquist and Majda is more accurate. All curves except that of Engquist and Majda show a linear attenuation rate, as expected for a single mode source. The oscillations in the attenuations predicted by the Engquist and Majda condition are typical of results obtained when the boundary is reflecting. Figures 5,6 and 7 show results for the same source and frequency, but when the boundary is located at $x = .8H$, $x = .6H$, and $x = .2H$, respectively. Although the attenuations are lower due to the shorter duct length, the trends are consistent with those

of figure 4. Note also that, as the boundary is brought closer to the source, the attenuation on a percentage basis is less accurate for all conditions except the nonlocal condition.

Attenuation predictions in figure 8, for which $L = H$ and the frequency is 1,000 Hz are typical of results obtained for several other duct lengths at that frequency. Here, the source is still the lowest order mode. At this higher frequency the liner is not effective, giving little attenuation over the lining. Both the Giles and the nonlocal condition gives accurate predictions but the condition of Engquist and Majda gives poor comparison with the modal series. Results were also computed for 5,000 Hz with the lowest order mode as the source and for several duct lengths. The attenuation curves are not shown in order to limit the amount of discussion. However, trends were consistent with that of figure 8.

Figure 9 shows results at a frequency of 100 Hz, $L = H$, and for the fifth order mode source. All boundary conditions give good predictions for $x/L < .75$. However, the condition of Engquist and Majda and also that of Giles gives poor attenuation predictions near the outflow boundary. In contrast, the nonlocal condition is in excellent agreement with the modal series in this region. The discrepancy in the attenuation predictions obtained with the other two boundary conditions was not eliminated by applying the boundary conditions closer to the source. To the contrary, the discrepancy on a percentage basis increased when the boundary was moved closer to the source. Further, predictions with the nonlocal condition were equally accurate when the boundary condition application point was moved close to the source.

Figure 10 shows the predictions at 1,000 Hz for the same source and duct length as figure 9. The boundary condition of Engquist and Majda gave poor predictions and this curve is not shown. The two remaining boundary conditions give accurate predictions, although the nonlocal condition is closer to the modal series results. Figure 11 shows predictions when the frequency is increased to 5,000 Hz and all boundary condition curves included. Note that the liner performs poorly at this frequency giving little attenuation. All boundary conditions give good predictions at this frequency. Note that the curve for the nonlocal condition and the modal series solution are identical.

It should be noted that in [7], results at a frequency of 5,000 Hz could not be accurately predicted using the nonlocal boundary condition. Further, it was speculated that the poor prediction at this frequency was a result of using only 3.4 points per axial wavelength. The banded solver adopted in this paper allows several hundred thousand degrees of freedom to be incorporated with relative ease. The good agreement with the modal series predictions at 5,000 Hz using the nonlocal boundary condition confirms that this conjecture was true.

Turbomachinery sources, such as aircraft engine fans, are distributed sources. Such sources contain acoustic energy in many duct modes. Figure 12 compares attenuation pre-

dictions for the distributed source define by (22) at a frequency of 100 Hz and for $L = H$. The nonlocal condition is generally the most accurate for this source. Further, the condition of Engquist and Majda gives attenuation predictions closer to the modal series results than the condition of Giles. Figure 13 shows results for the same source when the frequency is increased to 1,000 Hz. The curve generated by the Engquist and Majda condition is not shown, since it led to predictions ten decibels higher than the modal series results. Both the Giles and the nonlocal condition give nearly the same predictions, although the Giles condition is slightly more accurate in a small region near the end of the duct.

5 Concluding Remarks

Several non-reflecting boundary conditions which have potential application to duct acoustics have been evaluated for their effectiveness. Those that met the criteria and were tested are

1. The local boundary condition of Giles.

2. The local highly-absorbing boundary condition of Engquist and Majda.

3. The nonlocal boundary condition of Zorumski, Watson and Hodge.

The case of of an infinite two-dimensional duct without flow was used for simplicity. All three boundary conditions however, have extensions to three dimensionality, variable area and wall linings, and flow. The interior solution technique was a linear finite element method. All three boundary conditions were tested using the same grid and order of approximation. A band solver has been used to account for the large number of degrees of freedom required for high frequency and long ducts.

The effectiveness of each boundary condition has been evaluated by comparing predicted attenuation in a softwall duct with analytical results available from modal theory. All three boundary conditions were evaluated for the lowest order mode, a higher order mode, and for a distributed source. Attenuation predictions for several frequencies were evaluated, and the effects of applying each boundary condition close to the source has been investigated.

Results presented here show that the new nonlocal boundary condition of Zorumski, Watson, and Hodge gave results consistent with exact analytical predictions over a broad range of acoustic parameters. This boundary condition gave attenuation predictions more accurate than the condition of Giles and more accurate than the condition of Engquist and Madja over a range of acoustic parameters. Giles condition however, was competitive at higher frequencies where the liner was not effective. The boundary condition of Engquist and Majda gave poor predictions for the range of parameters considered. The accuracy of

the attenuation predictions on a percentage basis were observed to decrease with duct length when the Giles or condition of Engquist and Majda were used. However, the accuracy of the attenuation predicted using the nonlocal boundary condition is accurate for short ducts as well. This is an important result, since a substantial reduction in grid points can be obtained by applying the nonlocal condition close to the sound source. Implementation of the band solver has confirmed that the poor attenuation predictions at 5,000 Hz in the earlier paper is a result of having too few points per wavelength in the discretization.

6 References

References

[1] Engquist,Bjorn and Majda, Andrew., "Absorbing Boundary Conditions for the Numerical Simulation of Waves," *Mathematics of Computations*, Vol. 31, p. 629-651, 1977.

[2] Hedstrom, G.W., "Nonreflecting Boundary Conditions for Nonlinear Hyperbolic Systems," *Journal of Computational Physics*, Vol. 30, p. 222-237, 1979.

[3] Thompson, Kelvin W., "Time Dependent Boundary Conditions for Hyperbolic Systems," *Journal of Computational Physics*, Vol. 68, p. 1-28, 1987.

[4] Bayless, A. and Turkel,E., "Radiation Boundary Conditions for Acoustic and Elastic Wave Calculations," *Communications on Pure and Applied Mathematics*, Vol. 32, p. 312, 1979.

[5] Giles, M.B., "Nonreflecting Boundary Conditions for Euler Equation Calculations," *AIAA Paper 89- 1912*, CP, 1989.

[6] Watson, Willie R. and Myers, M.K., "Time Dependent Inflow-Outflow Boundary Conditions for 2-D Acoustic Systems," *AIAA Journal*, Vol. 29, no. 9, Sept. 1991 p. 1383-1389.

[7] Zorumski, W.E, Watson, W.R., and Hodge S.L., "A Non-reflecting Boundary Conditions for Duct Acoustics ," NASA TM109091, April, 1994.

[8] Eversman, W., "Energy Flow Criteria for Acoustic Propagation in Ducts with Flow," *Journal of the Acoustical Society of America*, Vol. 49, No. 6, June 1971.

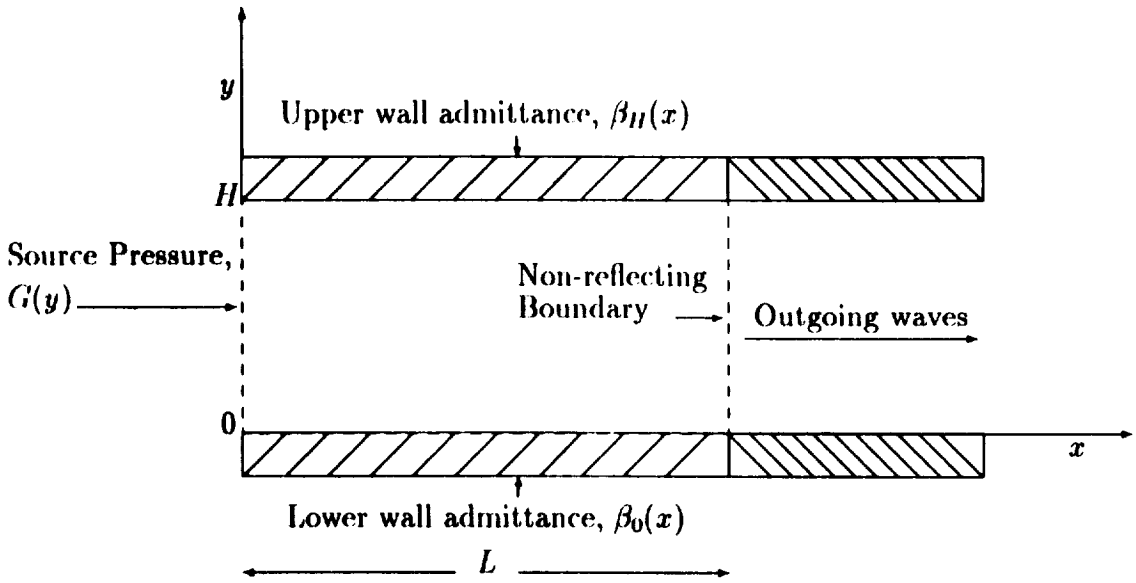

Figure 1: Two dimensional duct and coordinate system.

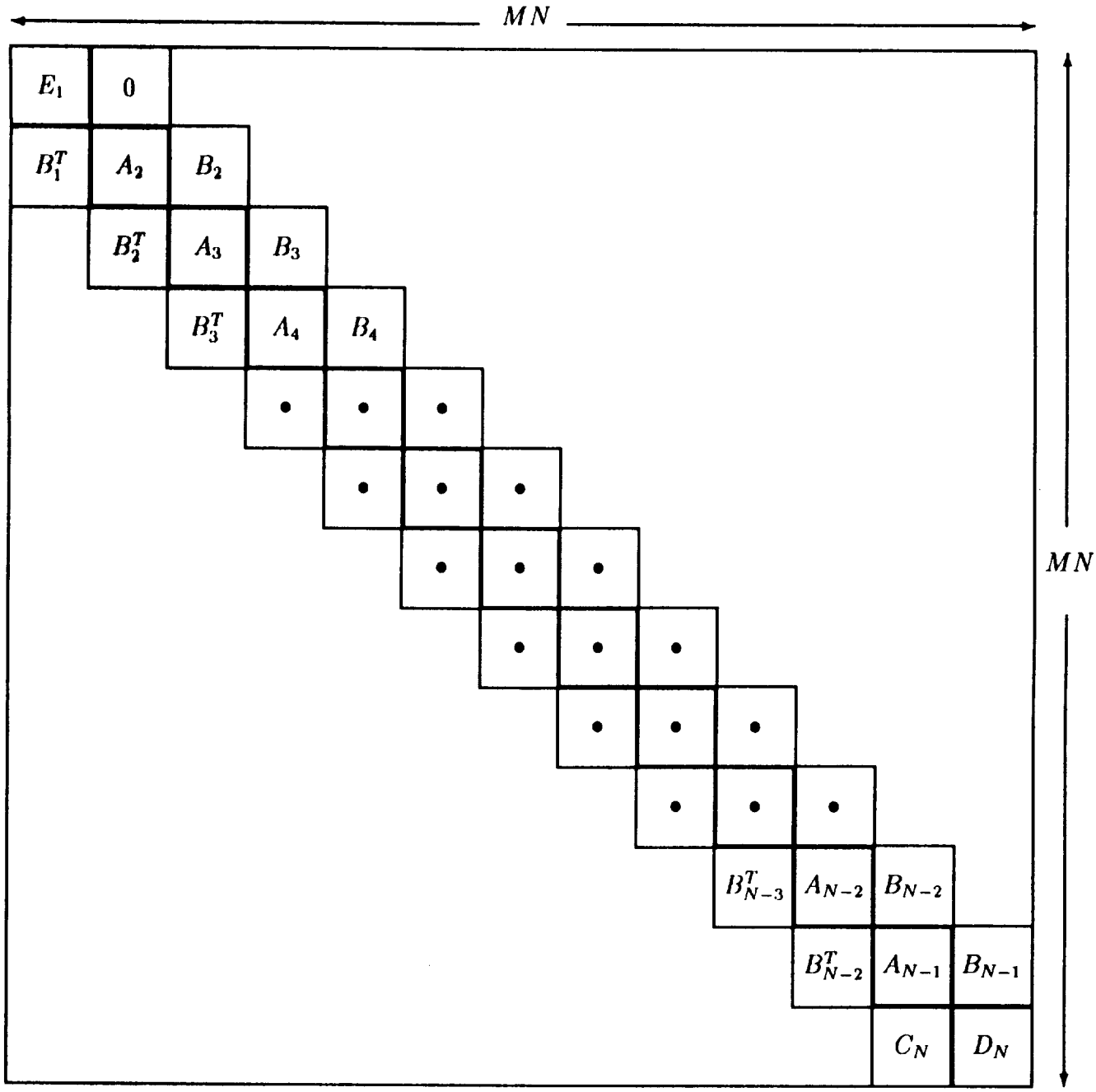

Figure 2: Structure of the global stiffness matrix, $[A]$, with minor blocks.

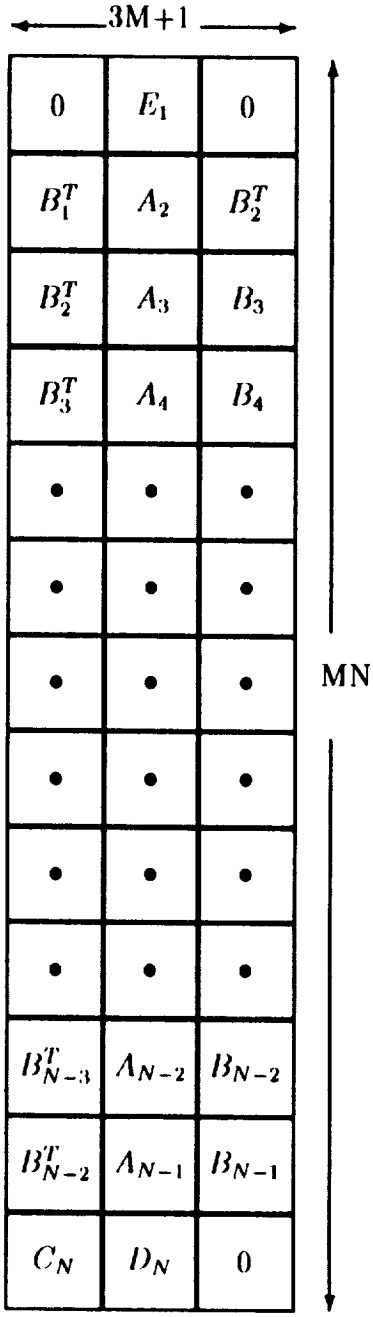

Figure 3: The stored MNx(3M+1)rectangular coefficient matrix with nonzero coefficients.

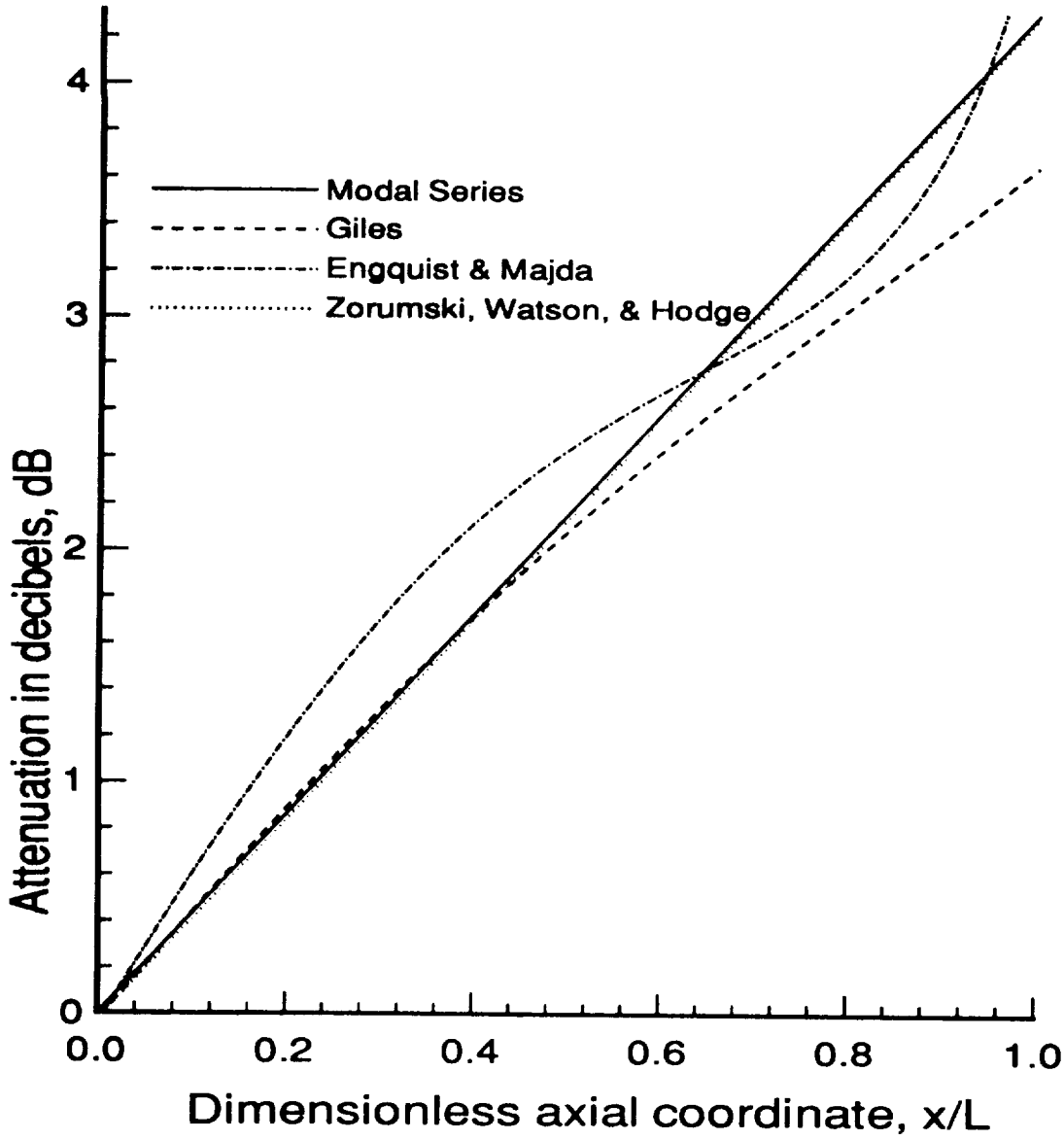

Figure 4: Attenuation comparison for the lowest order mode source in a softwall duct at 100 Hz (L=H).

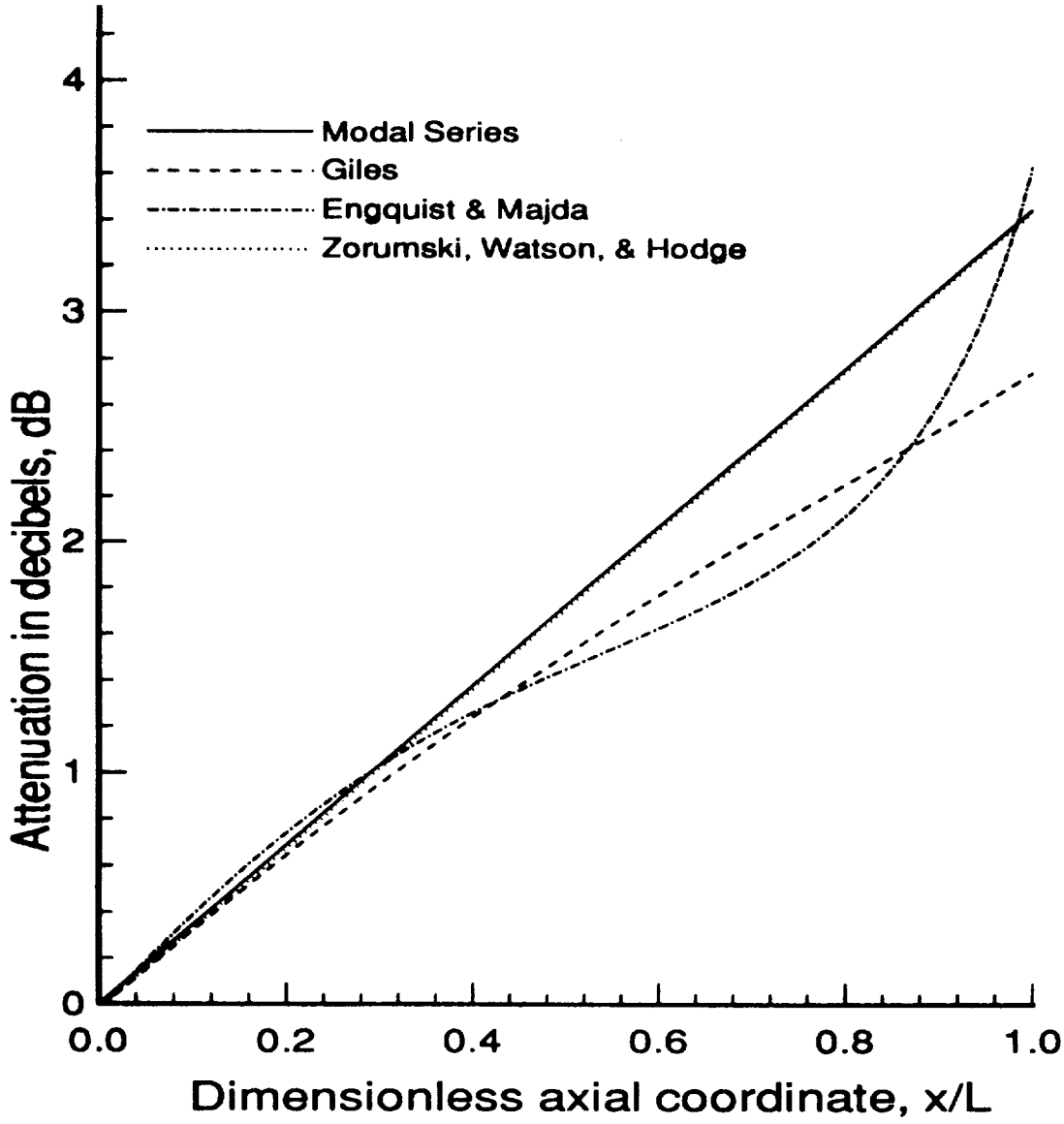

Figure 5: Attenuation comparison for the lowest order mode source in a softwall duct at 100 Hz ($L = .8H$).

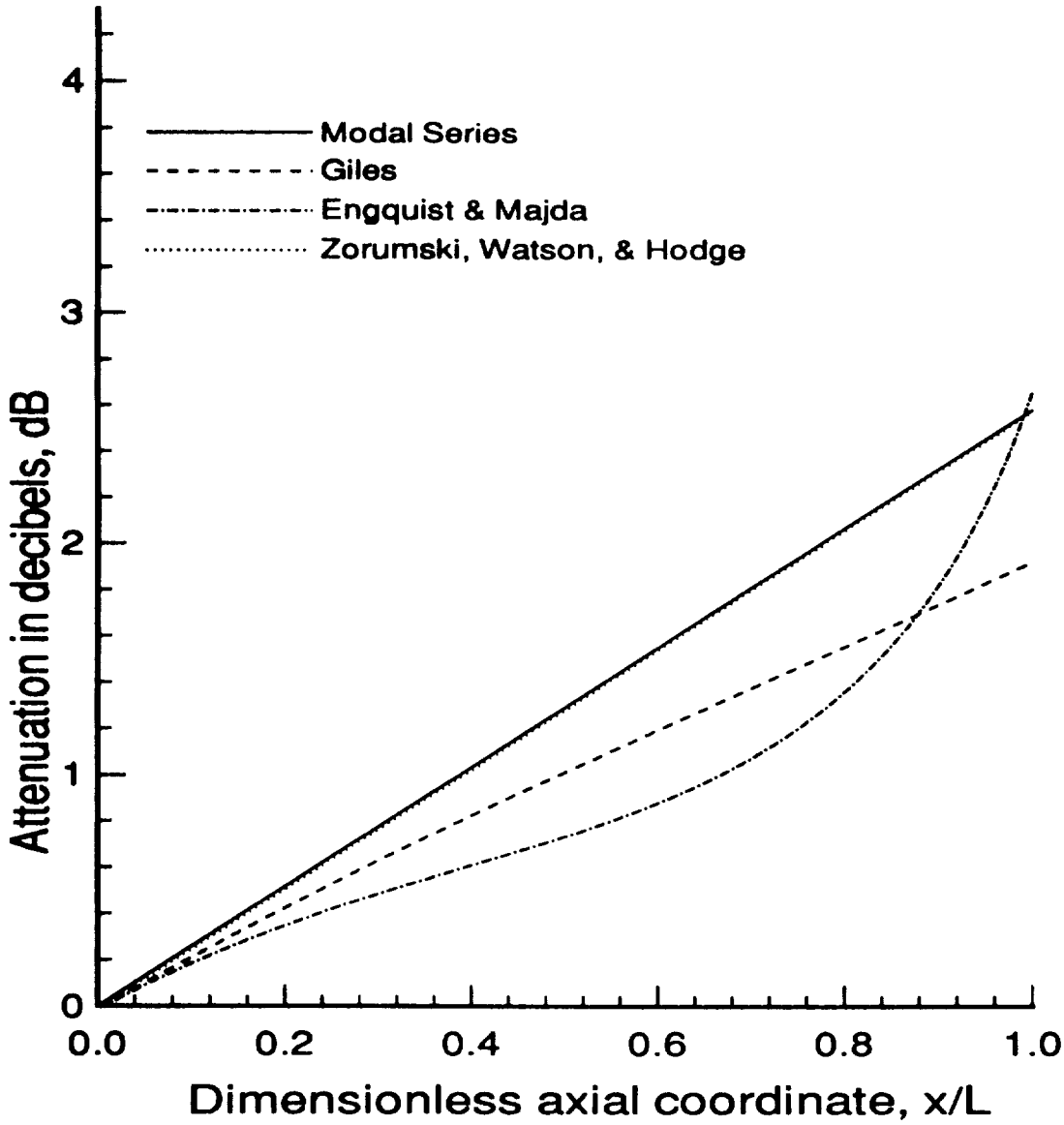

Figure 6: Attenuation comparison for the lowest order mode source in a softwall duct at 100 Hz ($L = .6H$).

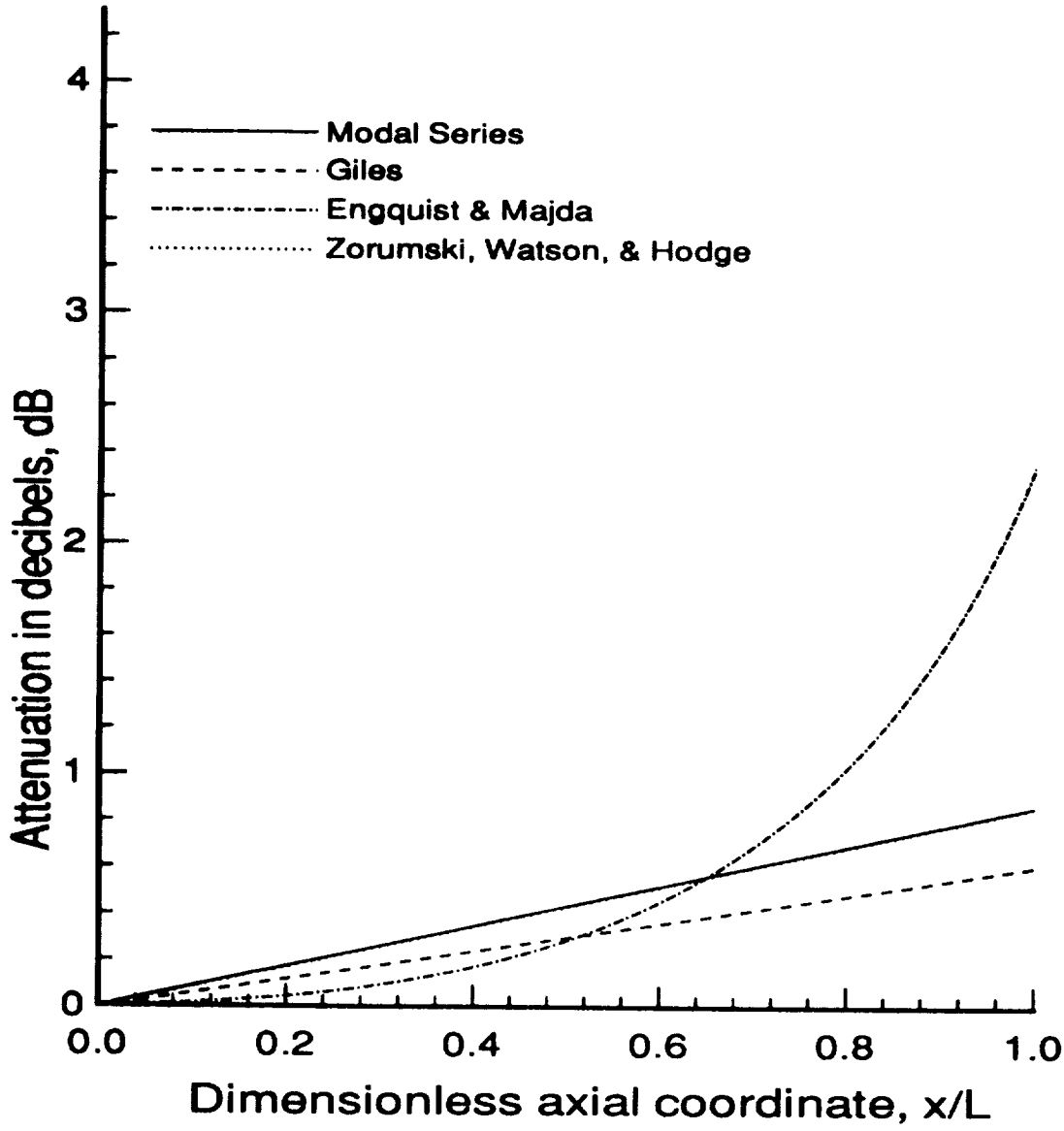

Figure 7: Attenuation comparison for the lowest order mode source in a softwall duct at 100 Hz ($L = .2H$).

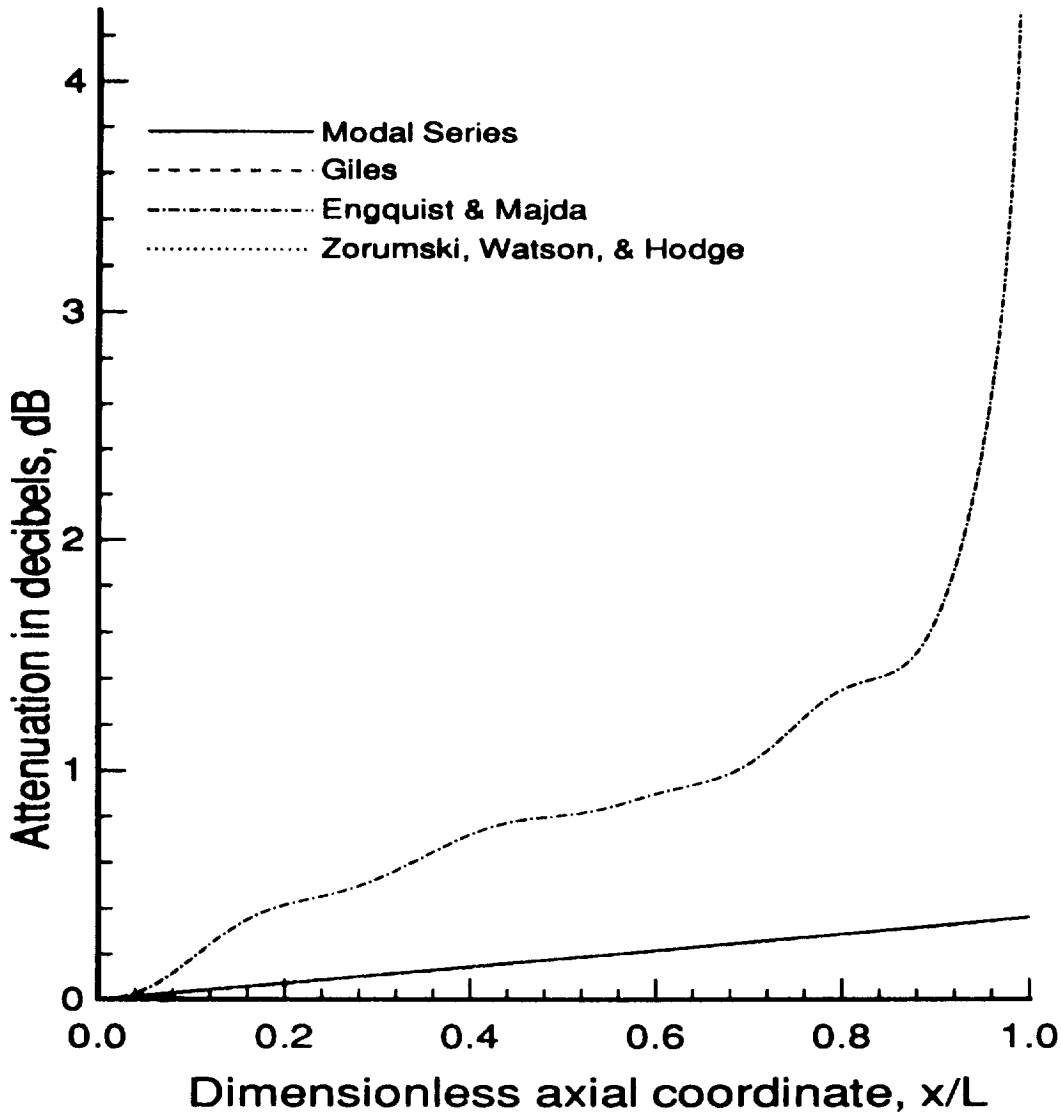

Figure 8: Attenuation comparison for the lowest order mode source in a softwall duct at 1,000 Hz ($L = H$).

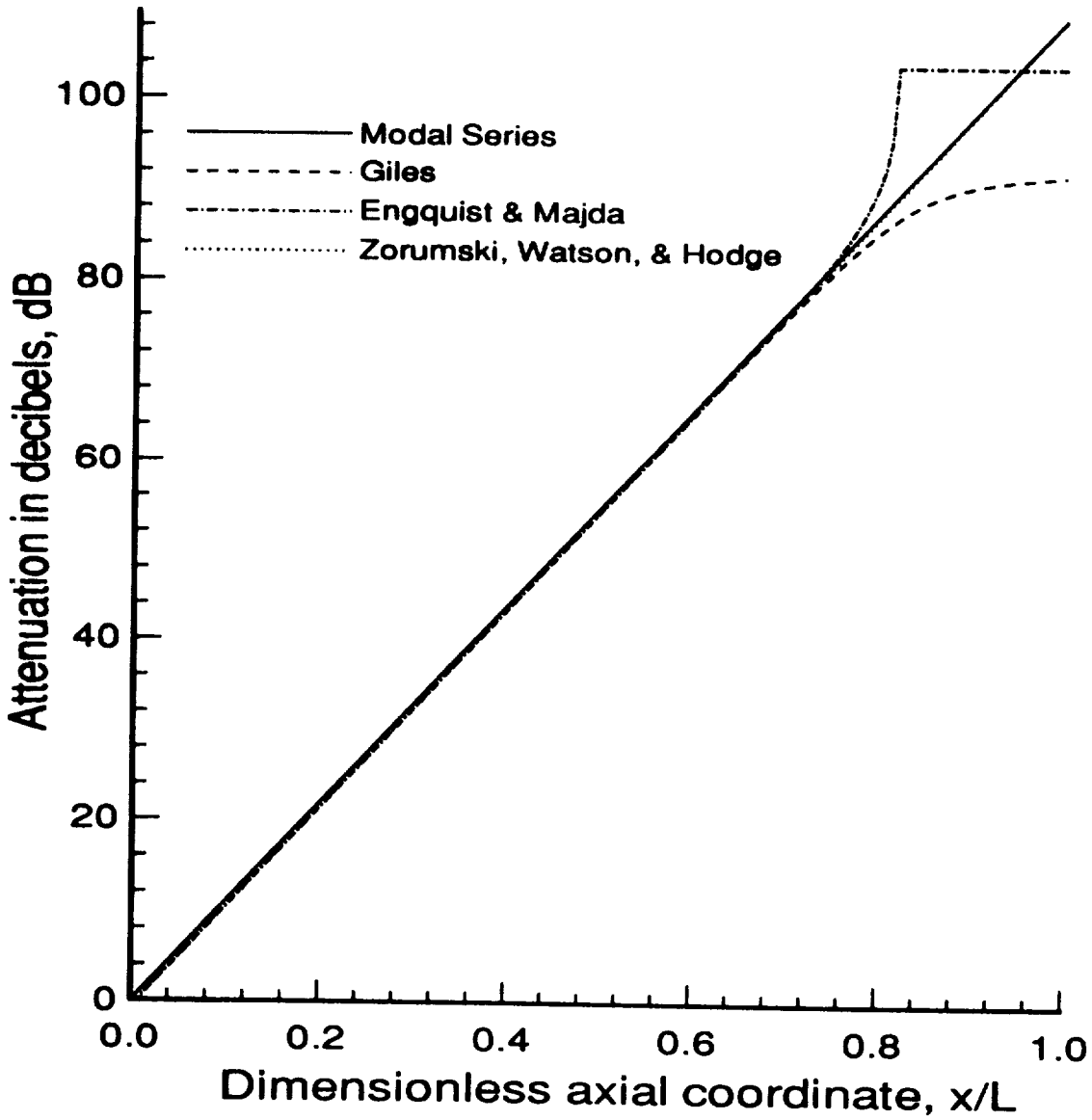

Figure 9: Attenuation comparison for the fifth order mode source in a softwall duct at 100 Hz ($L = H$).

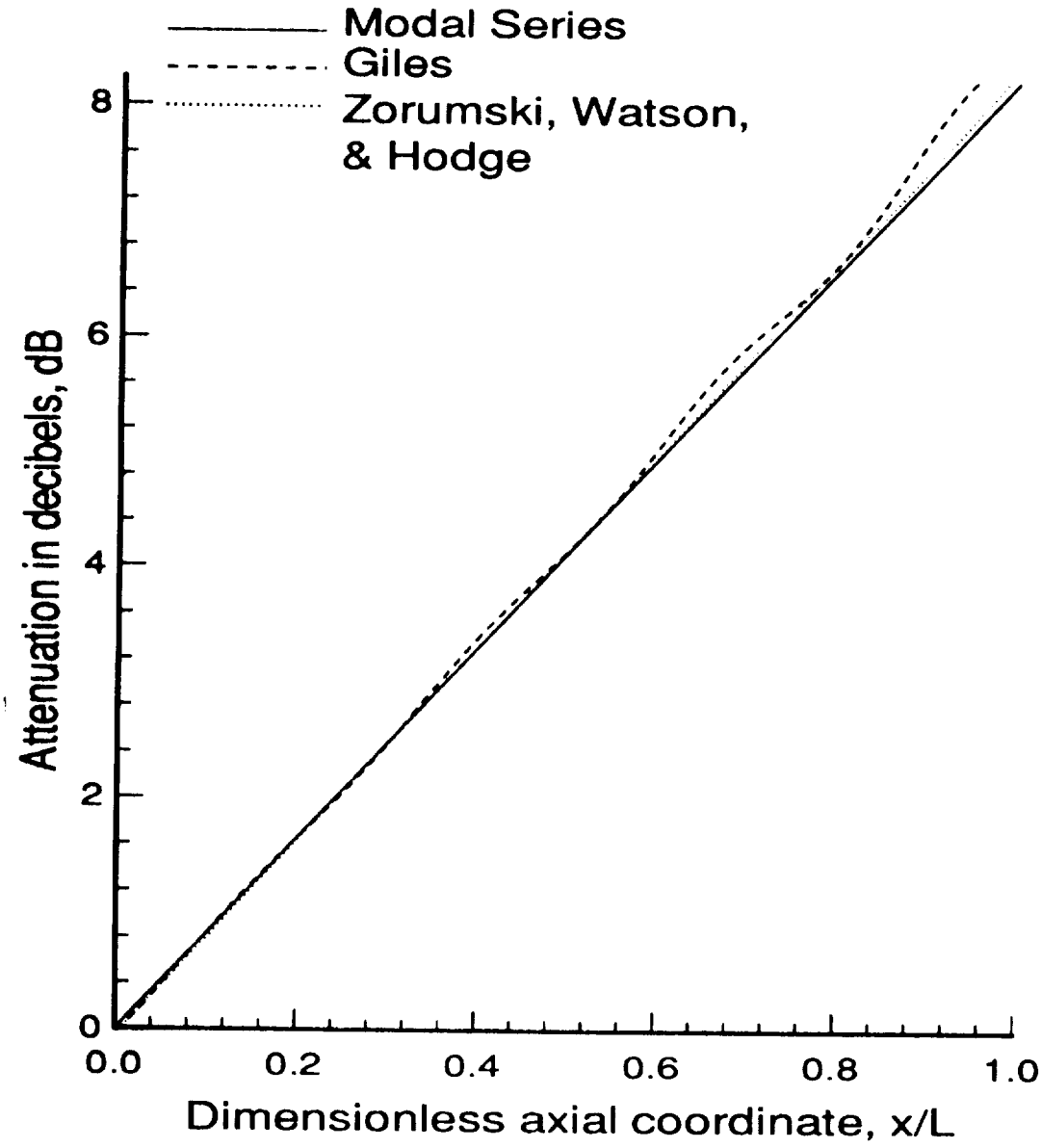

Figure 10: Attenuation comparison for the fifth order mode source in a softwall duct at 1,000 Hz ($L = H$).

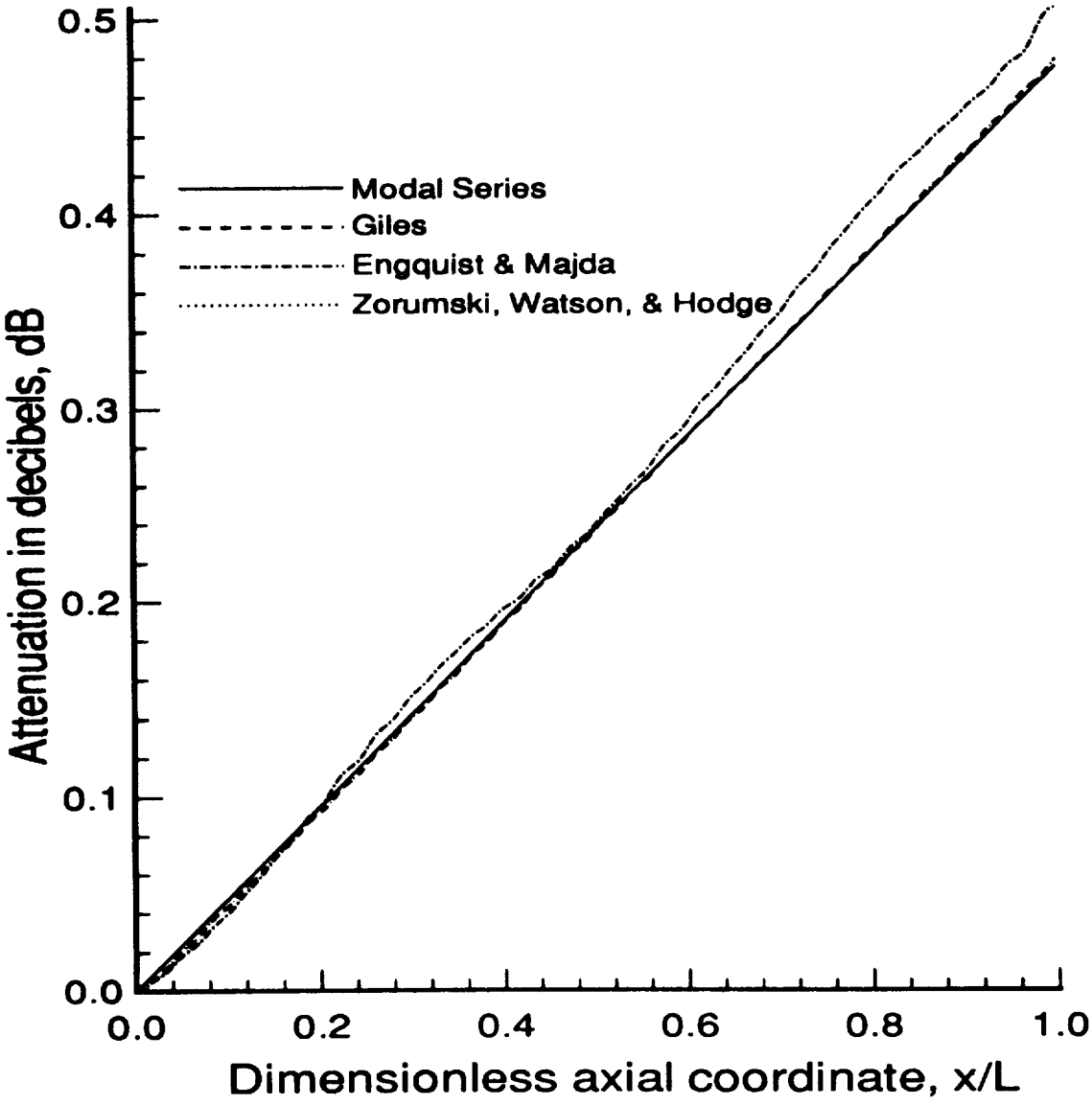

Figure 11: Attenuation comparison for the fifth order mode source in a softwall duct at 5,000 Hz ($L = H$).

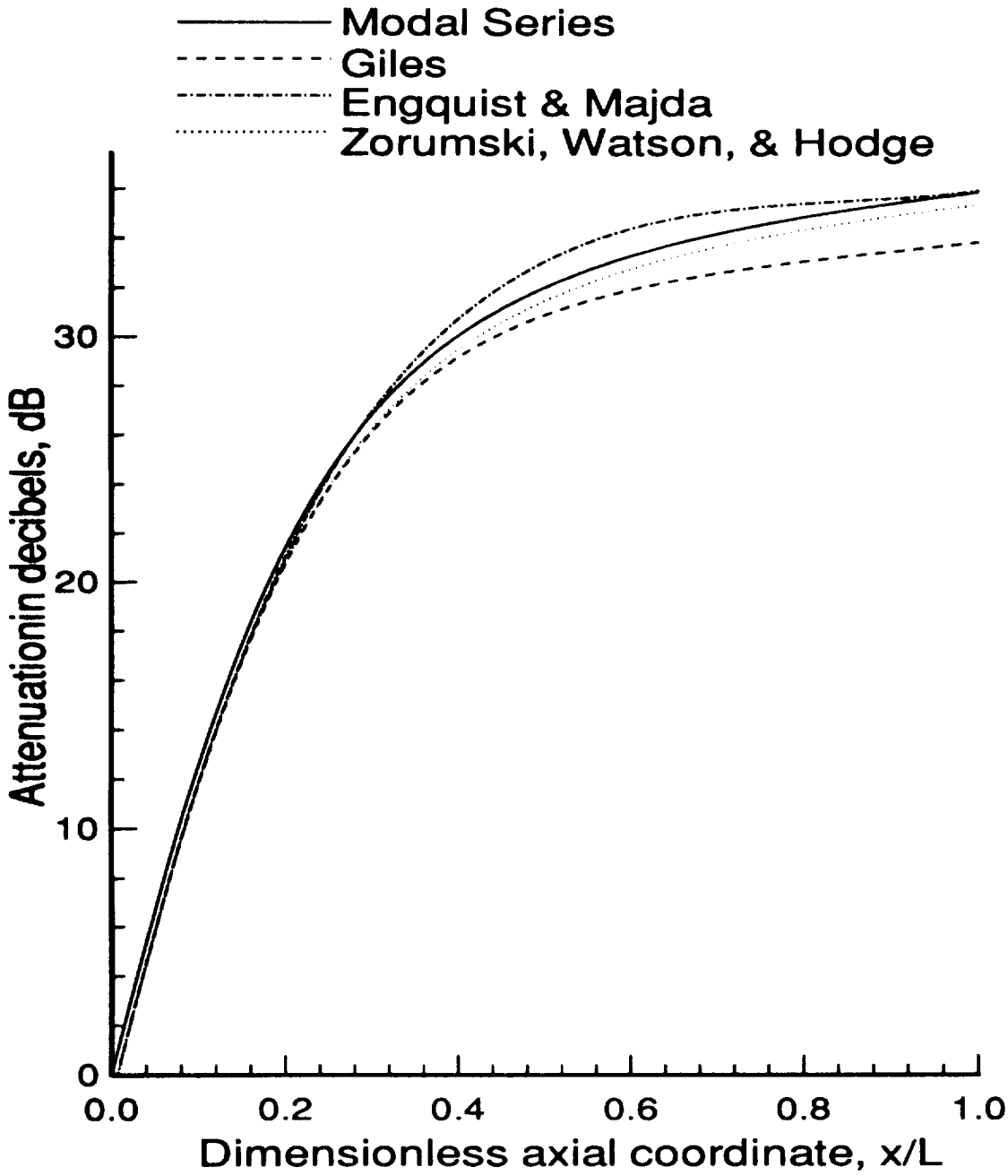

Figure 12: Attenuation comparison for a distributed source in a softwall duct at 100 Hz ($L = H$).

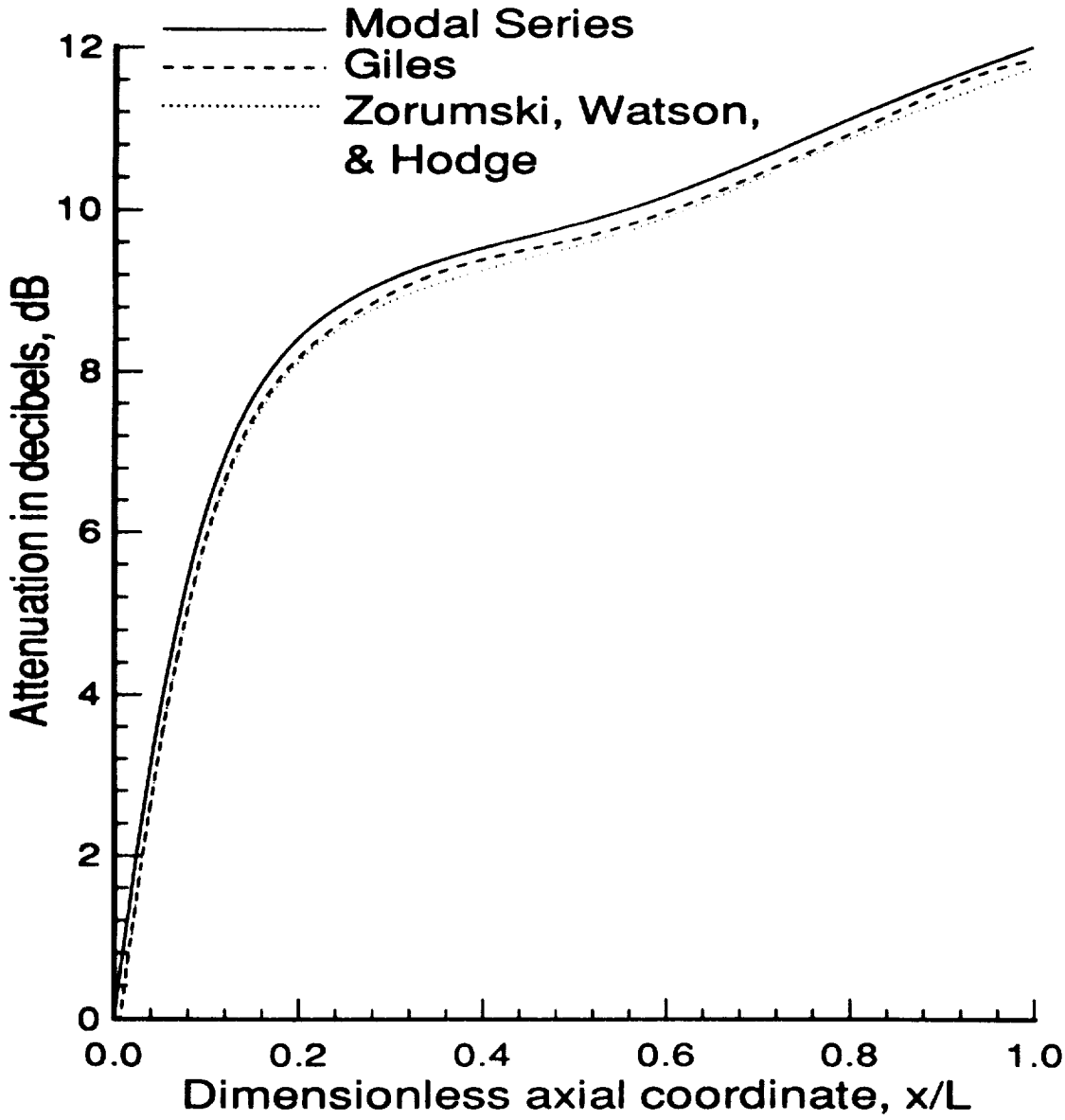

Figure 13: Attenuation comparison for a distributed source in a softwall duct at 1,000 Hz ($L = H$).

REPORT DOCUMENTATION PAGE

Form Approved
OMB No. 0704-0188

1. AGENCY USE ONLY *(Leave blank)*	2. REPORT DATE	3. REPORT TYPE AND DATES COVERED
	May 1994	Technical Memorandum

4. TITLE AND SUBTITLE
Evaluation of Several Non-reflecting Computational Boundary Conditions for Duct Acoustics

5. FUNDING NUMBERS
538-03-12-01

6. AUTHOR(S)
Willie R. Watson, William E. Zorumski, and Steve L. Hodge

7. PERFORMING ORGANIZATION NAME(S) AND ADDRESS(ES)
NASA Langley Research Center
Hampton, VA 23681-0001

8. PERFORMING ORGANIZATION REPORT NUMBER

9. SPONSORING / MONITORING AGENCY NAME(S) AND ADDRESS(ES)
National Aeronautics and Space Administration
Washington, DC 20546-0001

10. SPONSORING / MONITORING AGENCY REPORT NUMBER
NASA TM-109118

11. SUPPLEMENTARY NOTES
Watson and Zorumski: Langley Research Center, Hampton, VA
Hodge: Virginia Consortium of Engineering and Science Universities, Hampton, VA

12a. DISTRIBUTION / AVAILABILITY STATEMENT
Unclassified - Unlimited

Subject Category 71

12b. DISTRIBUTION CODE

13. ABSTRACT ***(Maximum 200 words)***

Several non-reflecting computational boundary conditions that meet certain criteria and have potential applications to duct acoustics are evaluated for their effectiveness. The same interior solution scheme, grid, and order of approximation are used to evaluate each condition. Sparse matrix solution techniques are applied to solve the matrix equation resulting from the discretization. Modal series solutions for the sound attenuation in an infinite duct are used to evaluate the accuracy of each nonreflecting boundary conditions. The evaluations are performed for sound propagation in a softwall duct, for several sources, sound frequencies, and duct lengths. It is shown that a recently developed nonlocal boundary condition leads to sound attenuation predictions considerably more accurate for short ducts. This leads to a substantial reduction in the number of grid points when compared to other nonreflecting conditions.

14. SUBJECT TERMS
Duct Liners; Computational boundary conditions; Non-reflecting boundary conditions; Finite element method; Helmholtz equation; Sparse marix technique

15. NUMBER OF PAGES
25

16. PRICE CODE
A03

17. SECURITY CLASSIFICATION OF REPORT	18. SECURITY CLASSIFICATION OF THIS PAGE	19. SECURITY CLASSIFICATION OF ABSTRACT	20. LIMITATION OF ABSTRACT
Unclassified	Unclassified		